Enhanced Reduced Order Model of Wind Turbines with DFIG for Power System Stability Studies

J.Kretschmann, H.Wrede, *Member, IEEE,* , S. Mueller-Engelhardt, I. Erlich, *Senior Member, IEEE*

Abstract **This paper presents an extension to the stability model of the doubly fed induction generator (DFIG) used for wind turbines. With the proposed extension it is possible to consider the alternating components of the rotor current and thus the variation of the converter DC-link voltage. With realistic DC-voltage responses, a more accurate modeling of crowbar switching will now be possible. The paper also presents suitable models for rotor and line side converters, as well as for the DC-link. Moreover, the paper provides simulation results not only for model verification but also for demonstrating the behavior of the DFIG and the corresponding control system during fault.**

***Index Terms*—Wind power, control system, power system stability, doubly-fed induction generator, crowbar**

I. NOMENCLATURE

$\underline{i}$, $\underline{u}$	complex current and voltage
l, x, r	inductance, reactance, resistance
$\underline{\Psi}$	complex flux-linkages
ω, s	angular speed, slip
t, T	Torque, time constant
Θ_m	Inertia of complete rotor shaft

subscripts

S, R	Stator, rotor
d, q	Direct, quadrature axis component
h, σ	Main field, leakage

Sign convention: consumed active power and inductive reactive power are considered positive

II. INTRODUCTION

THIS paper deals with the modeling of wind turbines equipped with doubly-fed induction generator (DFIG) in combination with static converter (dc-voltage link) and rotor side protection unit (crowbar) with a damping resistance connected in series. The basic structure is shown in Fig. 1. This variable-speed generator system permits the adjustment of rotor speed to match the optimum operating point depending on wind speed. This most commonly used system for wind power generation is characterized by high efficiency for the whole generator-converter-system.

J. Kretschmann, H. Wrede and S. Mueller-Engelhardt are with the SEG GmbH & Co. KG, 47906 Kempen, Germany,
(e-mail: j.kretschmann@newage-avkseg.com, h.wrede@newage-avkseg.com, s.mueller-engelhardt@newage-avkseg.com);
I. Erlich is with the University Duisburg-Essen, 47057 Duisburg, Germany
(e-mail: istvan.erlich@uni-due.de);

1-4244-0273-5/06/$20.00 ©2006 IEEE

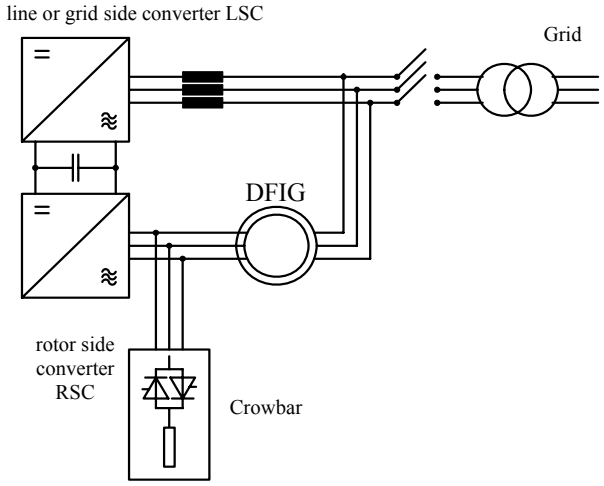

Fig. 1. Main components of the DFIG system

With the increasing share of wind turbines in electric power generation the dynamic behavior of the power system is impacted considerably. Therefore, many utilities have issued Grid Codes to define the basic requirement concerning wind turbine behavior during grid faults [1],[2]. The focus in this relation is directed at the fault ride through (FRT) capability and the voltage support to be provided by the wind turbines during fault. To prove conformity with grid requirements and to adapt control strategies to a particular grid, power system planners and grid operators need software tools and models representing wind turbines with sufficient accuracy. The challenge is to represent a large number of wind turbines in addition to conventional power plants connected to a large grid.

In [3] a reduced order model (ROM) for a DIFG is presented. This model allows the simulation of the operating performance of a large number of wind turbines (wind parks) connected to the power system. The presented model is based on neglecting the transformer terms in the stator and the grid on which the DFIG is operating. However, as a consequence of this simplification, the DC-components of stator current and stator flux are not contained in the corresponding solutions. On the other hand the stator DC- component has a fundamental influence on the behavior of the system. They result in alternating active power components on the rotor side which can lead to a fast rising voltage in the converter DC-link. When DC-link voltage exceeds a predefined limit, the crowbar has to be switched on for protection purposes. However, with the crowbar active, the DFIG operates as a

conventional slip-ring induction machine and can not be controlled by the rotor side converter. In this period the DFIG become a reactive power consumer.

One of the main objectives of this paper is to present a model extension to [3] which accounts for the neglected stator DC-components without increasing the modeling and simulation effort considerably. Thus the converter DC-circuit can be considered to represent the triggering of the crowbar firing more realistically. Simulation results at the end of this paper will show the dynamic performance of a typical wind energy DFIG system's response to a 3-phase grid fault, calculated using the improved model.

III. GENERATOR (DFIG): BASIC MODEL

The reduced order model of the DFIG is summarized below. More detailed description is given in [3].

The fundamental system of equations for the DFIG is given by:

Voltage equations:

$$\underline{u}_S = r_S \underline{i}_S + \frac{d\underline{\psi}_S}{dt} + j\omega_S \underline{\psi}_S \tag{1}$$

$$\underline{u}_R = r_R \underline{i}_R + \frac{d\underline{\psi}_R}{dt} + j(\omega_S - \omega_R)\cdot \underline{\psi}_R \tag{2}$$

Flux equations:

$$\underline{\psi}_S = (l_h + l_{\sigma S})\underline{i}_S + l_h \cdot \underline{i}_R \tag{3}$$

$$\underline{\psi}_R = l_h \underline{i}_S + (l_h + l_{\sigma R})\underline{i}_R \tag{4}$$

Equation of motion

$$\frac{d\omega_R}{dt} = \frac{1}{\theta_m}\left(t_m + \mathrm{Im}[\underline{\psi}_S^* \underline{i}_S\right) \tag{5}$$

The orthogonal dq-reference frame used in this description is rotating at the speed ω_S.

After some algebraic manipulation one obtains the complex state equation for the electrical stator and rotor circuits,

$$\frac{d\underline{\psi}_S}{dt} = \left(-\frac{r_s(l_h + l_{\sigma R})}{l_h(l_{\sigma S} + l_{\sigma R}) + l_{\sigma S} l_{\sigma R}} - j\omega_S\right)\underline{\psi}_S + \frac{l_h r_s}{l_h(l_{\sigma S} + l_{\sigma R}) + l_{\sigma S} l_{\sigma R}}\underline{\psi}_R + \underline{u}_S \tag{6}$$

$$\frac{d\underline{\psi}_R}{dt} = \frac{r_R l_h}{l_h(l_{\sigma S} + l_{\sigma R}) + l_{\sigma S} l_{\sigma R}}\underline{\psi}_S - \left(\frac{r_R(l_h + l_{\sigma S})}{l_h(l_{\sigma S} + l_{\sigma R}) + l_{\sigma S} l_{\sigma R}} + j(\omega_S - \omega_R)\right)\underline{\psi}_R + \underline{u}_R \tag{7}$$

which, together with the equation of motion (5), form the full order model (FOM) that can be used for instantaneous value, dynamic time domain simulations. Often the stator voltage is considered constant or interpreted as an independent input variable. That allows using the FOM for the study of a single machine operating on an infinite bus. However, the stator voltage can vary according to the type of interaction between DFIG and the grid. Basically FOM requires differential equations for the whole network due to the fact that the grid is directly connected to the stator circuit. Using the differential equations of the grid, the stator voltage in (6) can be eliminated. If the FOM is used for time domain simulation small integration step sizes are required due to the small time constants involved. The small integration time step, in addition to the large number of differential equations especially for the grid, results in considerable simulation efforts when studying large systems. These disadvantages limit the application of the FOM to small grids or even to a single machine, infinite bus systems.

A reduced order model (ROM) can be derived by neglecting the derivative term in the stator equation, i.e. by setting $\frac{d\underline{\psi}_S}{dt} = 0$.

In the strict sense, this approximation is only warranted in a reference frame rotating at a speed close to the synchronous speed $\omega_0 = 1.0\,p.u.$. The transformation of (6) and (7) into a synchronously rotating reference frame results in the transition $\omega_S \to \omega_0$. The ROM of the DFIG derived in [3] is described by an algebraic equivalent circuit shown in Fig. 2 where the transient impedance $\underline{z}'$ is defined as:

$$\underline{z}' = r_s + jx' = r_s + j\omega_0\left(l_h + l_{\sigma S} - \frac{l_h^2}{l_h + l_{\sigma R}}\right) \tag{8}$$

The Thevenin voltage source $\underline{u}'$ behind the impedance $\underline{z}'$ is a function of the state variable rotor flux

$$\underline{u}' = j\omega_0 k_R \underline{\psi}_R \tag{9}$$

With $k_R = \frac{l_h}{l_h + l_{\sigma R}}$

To consider the time behavior of the rotor flux the following differential equation has to be solved:

$$\frac{d\underline{\psi}_R}{dt} = \left(-\frac{r_R}{l_h + l_{\sigma R}} + j(\omega_0 - \omega_R)\right)\underline{\psi}_R + k_R r_R \underline{i}_S + \underline{u}_R \tag{10}$$

Furthermore, the model has to be extended by the equation of motion that is also adapted according to the model reduction introduced.

$$\frac{d\omega_R}{dt} = \frac{1}{\theta_m}\left(t_m + \mathrm{Im}\left[k_R \underline{\psi}_R^* \underline{i}_S\right]\right) \tag{11}$$

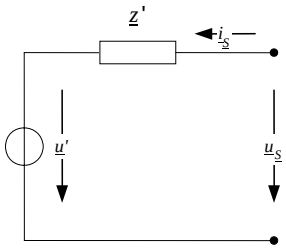

Fig. 2. Equivalent circuit of the reduced order DFIG model

In the ROM the stator flux is no more a state variable and therefore, can change instantaneously. Concerning the rotor flux behavior, the approximation introduced is clearly justified when the crowbar is not switched on (see upper part of Fig. 3). However, with the crowbar active, the rotor flux contains considerable alternating components not covered by the ROM.

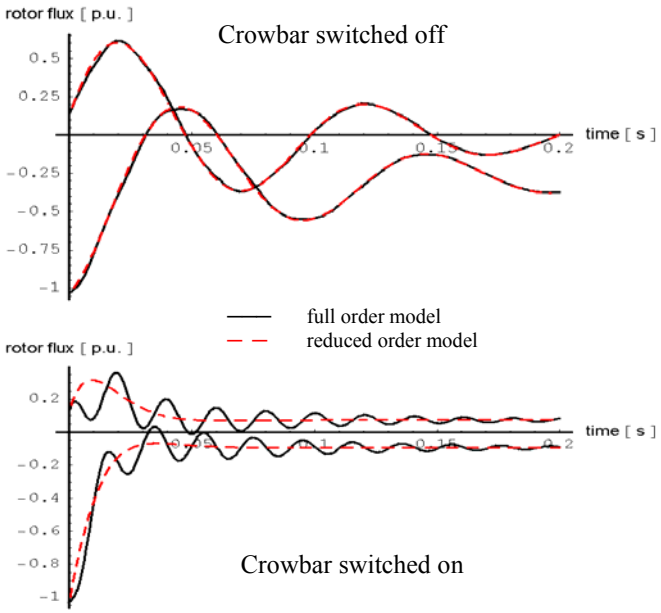

Fig. 3. Rotor flux-components Ψ_{Rd}, Ψ_{Rq}, caused by a three-phase voltage sag to 15 %

IV. Enhanced Generator (DFIG) Model

In a practical situation, DC-components can appear on both stator and rotor sides, which can only be captured by the FOM. They generate an alternating active power resulting in fast rise of the DC-link voltage and subsequently can lead to crowbar switching. Because the DC-components are not part of the ROM solution, this model (ROM) doesn't provide correct information for initializing crowbar control. For this purpose an enhanced model is proposed in this paper which still allows the use of the ROM, but activates an additional model part to add the DC-components to the simulation results as necessary.

The idea is based on the assumption that the stator flux calculated using the ROM is just the slow component of $\underline{\Psi}_S$.

From (6) follows with $\frac{d\underline{\Psi}_S}{dt} = 0$

$$0 = \left(-\frac{r_s(l_h + l_{\sigma R})}{l_h(l_{\sigma S} + l_{\sigma R}) + l_{\sigma S} l_{\sigma R}} - j\omega_0\right)\underline{\Psi}_S^{ROM} + \frac{l_h r_s}{l_h(l_{\sigma S} + l_{\sigma R}) + l_{\sigma S} l_{\sigma R}}\underline{\Psi}_R^{ROM} + \underline{u}_S^{ROM} \quad (12)$$

where the superscript "ROM" signifies the slow ROM solution. In synchronous reference frame subtracting (18) from (6) results in

$$\frac{d\underline{\tilde{\Psi}}_S}{dt} = \left(-\frac{(r_s + r_N)(l_h + l_{\sigma R})}{lh\,(l_{\sigma S} + l_N + l_{\sigma R}) + (l_{\sigma S} + l_N) l_{\sigma R}} - j\omega_0\right)\left(\underline{\tilde{\Psi}}_S - \underline{\Psi}_S^{ROM}\right) \quad (13)$$

under the following assumptions:

1) $\underline{\Psi}_R \approx \underline{\Psi}_R^{ROM}$ This is nearly fulfilled when the crowbar is switched off (see Fig.3). With crowbar this assumption is less tenable but still acceptable.

2) $\underline{u}_S = \underline{u}_S^{ROM}$ This presupposes that the stator terminal is extended up to the Thevenin equivalent voltage of the grid $\underline{u}_{SN}$ in accordance with Fig. 4. In this case the stator parameters must be also modified as $r_S \to r_S + r_N$ and $l_{\sigma S} \to l_{\sigma S} + l_N$. However, it should be emphasized that it is not necessary to know $\underline{u}_{SN}$ specifically, but the assumption must be, in principle, possible. The corresponding equivalent grid impedance is easily calculated from the well known short circuit capacity S_k''. It is obvious that the suggested extension of the stator circuits to a virtual voltage source corresponds with the assumptions used for the standard short-circuit current calculation. However, the approach presupposes a constant equivalent grid impedance. Therefore, the simulation is restricted to cases where the impedance is not significantly effected by the grid fault.

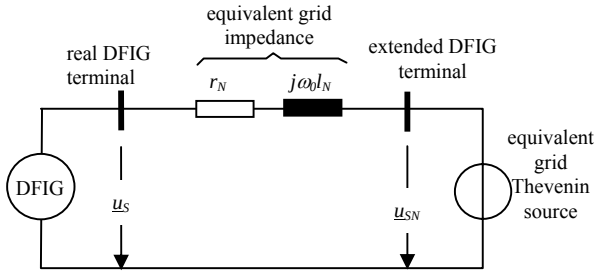

Fig. 4 Extension of the DFIG terminal

In (13) the stator flux is given as $\underline{\tilde{\Psi}}_S$ to indicate the approximation used as well as the extension of the stator through the grid equivalent. Equation (13) has only the input variable $\underline{\Psi}_S^{ROM}$ that is calculated by

$$\underline{\Psi}_S^{ROM} = \left(x' + \omega_0 l_N\right)\underline{i}_S^{ROM} + k_R \underline{\Psi}_R^{ROM} \quad (14)$$

and so (13) can be solved parallel to the ROM equation system as shown in Fig. 5.

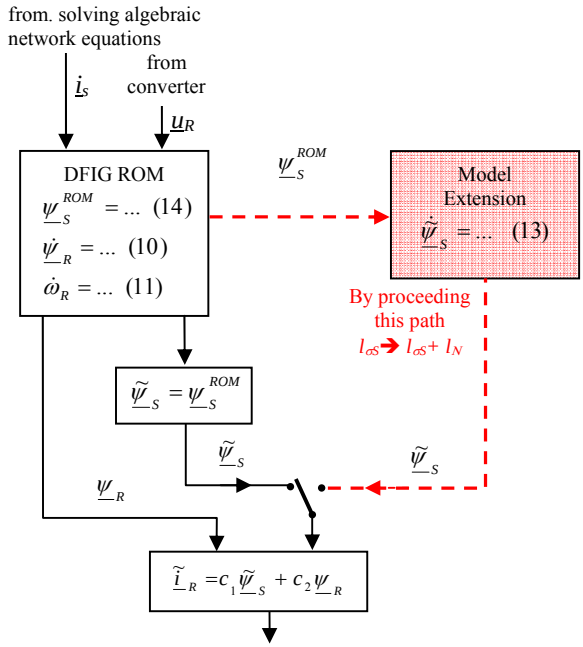

Fig. 5. Simulation algorithm using ROM extension

The coefficients c1 and c2 follow from (3) and (4):

$$c_1 = -\frac{l_h}{l_h(l_{\sigma S}+l_N+l_{\sigma R})+(l_{\sigma S}+l_N)l_{\sigma R}} \tag{15}$$

$$c_2 = \frac{l_{\sigma S}+l_h}{l_h(l_{\sigma S}+l_N+l_{\sigma R})+(l_{\sigma S}+l_N)l_{\sigma R}} \tag{16}$$

Notice that the network equivalent inductance l_N is zero when only the standard ROM model is used. The model extension has to be considered just following grid faults and can be disregarded when the difference between $\underline{\tilde{\psi}}_S$ and $\underline{\psi}_S^{ROM}$ is negligible.

The ROM with the proposed extension (ROM/E) allows the calculation of the rotor currents including the corresponding alternating components. Fig. 6 demonstrates the accuracy.

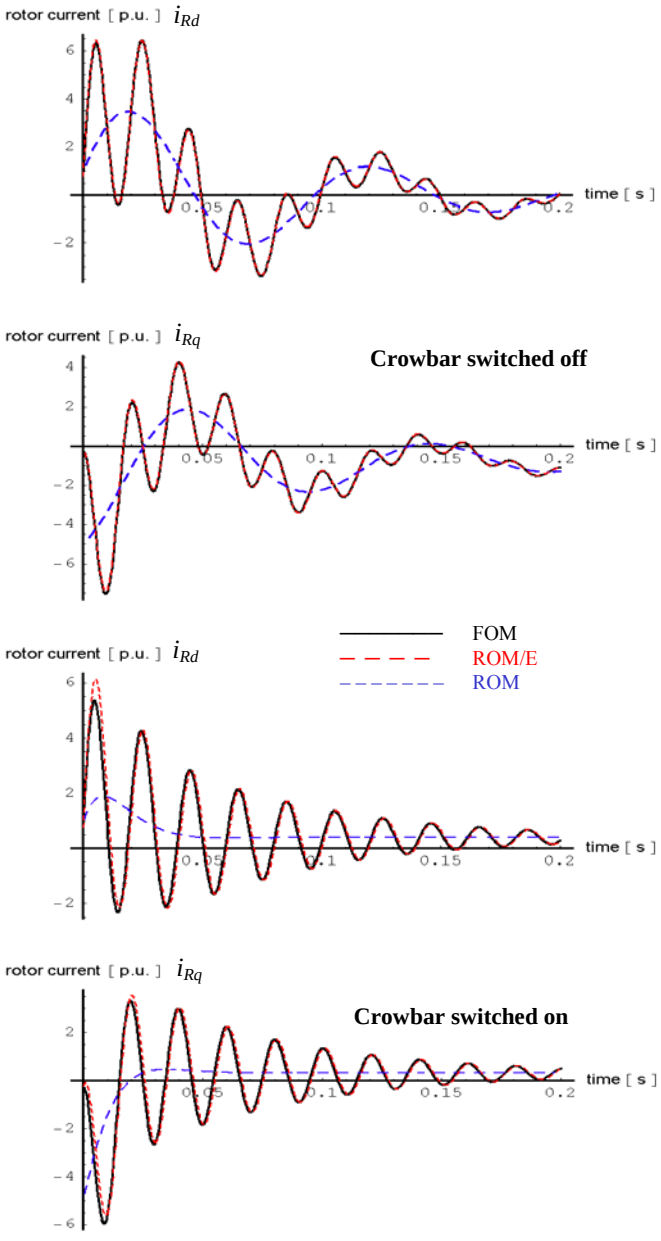

Fig. 6. Rotor currents following a three-phase voltage sag from rated voltage down to 15 %,

The ROM/E model provides very accurate results when the crowbar is not included. Actually, no difference between FOM and ROM/E results is observable in Fig. 6. With crowbar the difference between FOM and ROM/E is already visible but still acceptable from practical point of view. The impairment of model accuracy is evident, when one considers the fact that the rotor resistance increases when the crowbar is switched on. Thus the characteristic speed difference between the fast stator and the slow rotor flux is reduced, which is the physical basis for model reduction and so for the derivation of the ROM.

The ROM/E can be interpreted as an approximation of the full order DFIG model, but without using differential equations for the whole network. The integration step size required for ROM/E is usually smaller than that using the ROM only. However, the model extension is necessary only temporarily and therefore the integration step size can be increased when the model is switched back from ROM/E to ROM.

V. Model of the Rotor Side Converter and DC-Link

A realistic simulation of the crowbar action requires modeling of the converter DC-circuit because the triggering signal is typically derived from the DC-voltage. The DC-circuit contains a capacitor which is charged/discharged by the rotor and grid side converter currents, respectively. However, the capacitor is usually not big enough for smoothing the DC-voltage variations caused by the alternating rotor current. Therefore, accurate rotor currents are the pre-requisite for modeling of crowbar switching. In some applications the converter DC-link is extended by a chopper to keep the DC-voltage within limits thereby reducing the number of the crowbar actions or even under circumstances forestalling crowbar action altogether.

The time behavior of the converter DC-voltage can be described by the following equation:

$$\frac{du_{DC}}{dt} = \frac{\Delta p_{DC}}{u_{DC}\cdot c_{DC}} \tag{17}$$

where

$$\Delta p_{DC} = p_{RSC} + p_{LSC} + p_{Chopper} - p_{RSC\_losses} - p_{LSC\_losses} \tag{18}$$

with

$$p_{RSC} = -(u_{Rd}i_{Rd} + u_{Rq}i_{Rq})$$

$$p_{LSC} = u_{LSC,d}i_{LSC,d} + u_{LSC,q}i_{LSC,q}$$

$$p_{Chopper} = -\frac{u_{DC}^2}{r_{Chopper}} \qquad \textit{chopper switched on}$$

$$p_{Chopper} = 0 \qquad \textit{chopper switched off}$$

The chopper is active when the DC-voltage exceeds a predefined threshold. The converter losses are usually small (approximately 1% of rated output power) and therefore, negligible for the desired stability type of simulations. However, for higher accuracy requirements a polynomial approach is applicable for both RSC and LSC as well

$$p_{x\_losses} = p_{x0} + a_{x1}|i_x| + a_{x2}|i_x|^2 \quad (19)$$

where the index "x" stands for RSC or LSC respectively.

For considering the full extent of the interaction between DFIG and rotor side converter, one has to distinguish between four operating modes (see Fig. 7). The transition logic between the modes is shown in Fig. 8.

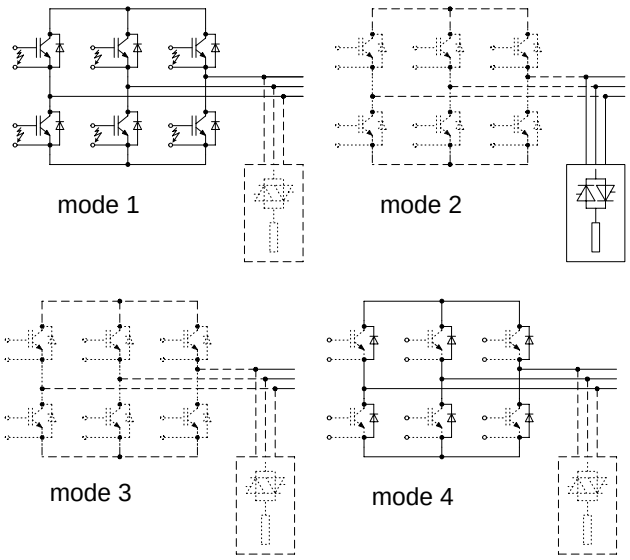

Fig. 7. Operating modes of the DFIG rotor side converter

Logic operation					
Crow ON	RSC ON	Diode ON	Diode OFF	OP_Mode Memory =4?	Output
0	0	0	0	0	3
0	0	0	0	1	4
0	0	0	1	0	3
0	0	0	1	1	3
0	0	1	0	0	3
0	0	1	0	1	4
0	0	1	1	0	4
0	0	1	1	1	3
0	1	0 or 1	0 or 1	0 or 1	1
1	0	0 or 1	0 or 1	0 or 1	2
1	1	0 or 1	0 or 1	0 or 1	2

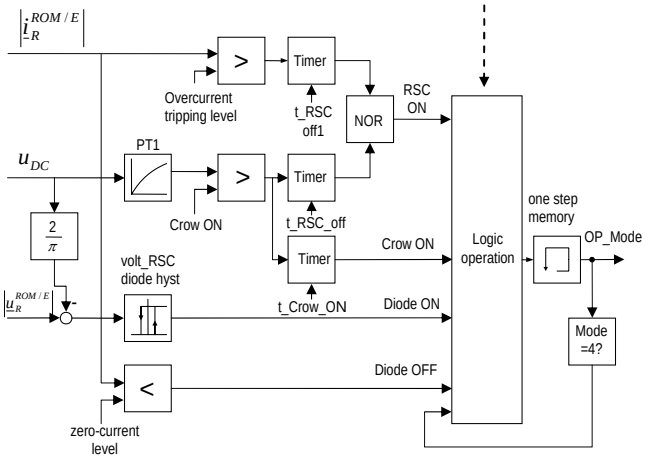

Fig. 8. Switching logic between different operating modes

Mode 1): Normal mode. Rotor current and rotor voltage are controlled by the IGBT's.

Mode 2): Crowbar mode. Rotor side IGBT-converter switched off, crowbar switched on.

When the crowbar is on, the DFIG equations have to be solved with

$$\underline{u}_R = 0$$

$$r_R \rightarrow r_R + r_{Crowbar}$$

The rotor side converter controller is stopped and reset in this mode.

Mode 3): No load mode; rotor side IGBT-converter switched off; rotor-current $\underline{i}_R = 0$

In this mode the rotor flux follows the stator current according to (4) instantaneously and therefore $\underline{\Psi}_R$ doesn't constitute a state variable when the rotor circuits are open. In fact, based on the assumption $\underline{i}_R = 0$ the model described above should be changed considerably for mode 3. However, it is possible to keep the model structure unchanged by using the following approximation:

$$\frac{d\underline{\psi}_R^{ROM}}{dt} = -\frac{1}{T}\left(\underline{\psi}_R^{ROM} - l_h \underline{i}_S^{ROM}\right) \quad (20)$$

where the fictive time constant T must be chosen small for guaranteeing a good approximation of real undelayed behavior. Simulation results shown at the end of this paper have been calculated with T= 1 ms. Due to $\underline{i}_R = 0$, eq. (13) has to be modified too.

$$\frac{d\tilde{\underline{\psi}}_S}{dt} = \left(-\frac{r_s + r_N}{l_h + l_{\sigma S} + l_N} - j\omega_0\right)\left(\tilde{\underline{\psi}}_S - \underline{\psi}_R^{ROM}\right) \quad (21)$$

Mode 4): Deactivated IGBT-converter mode (rotor side IGBT-converter switched off caused by over-current); generator rotor windings are fed by anti-parallel diodes of rotor side converter. Fast rise of the DC-link voltage is possible.

In mode 4 the DFIG can be described by the same equations as used for normal mode. However, the absolute value of rotor voltage is determined by the DC-link voltage only. The phase angle of $\underline{u}_R$ always corresponds with the phase angle of the rotor current (power factor = 1.0).

$$\underline{u}_R = \frac{2u_{DC}}{w_{21}\pi} \cdot e^{-j\arg(\underline{i}_R)} \quad (22)$$

where w_{21} considers the turn ratio between the reference values of u_{DC} and $\underline{u}_R$.

VI. Model of the Rotor side Converter

Detailed description of the model for the control system is presented in [3]. As a compendium block diagrams are shown in Fig. 9 and 10. The set-values of rotor current are calculated directly from set-values of active and reactive power. The rotor side converter is prevented from overload by limiting the magnitude of rotor-current set values.

The upper index $\angle u_S$ indicates the orientation of the dq-coordinate system on the stator voltage $\underline{u}_S$ that is measured in

a common synchronously rotating reference frame. In particular, this means that the d-axis always corresponds with the direction of the stator voltage.

Fig. 10 shows the rotor current control loops. PI-controllers are used for fast injection of the required rotor current. Often the dotted cross-coupling terms are neglected. However, due to the possible accuracy improvement and the fact that the additional effort is limited, it is recommended to consider the cross-coupling terms.

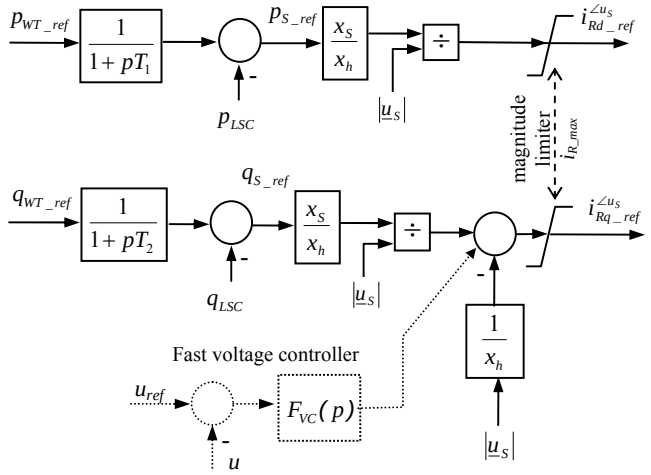

Fig. 9. Block diagram for the calculation of rotor current set values

The slip "s" relates in this description to the synchronously rotating common reference frame with $\omega_0 = 1.0\ p.u.$. Thus,

$$s = \frac{\omega_0 - \omega_R}{\omega_0} \tag{23}$$

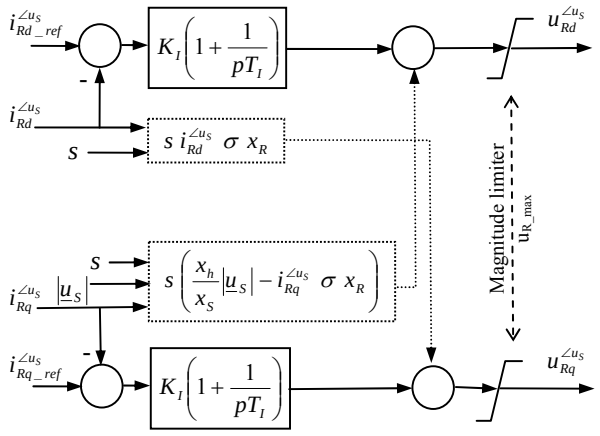

Fig. 10. Block diagram of rotor-current control-system

VII. Model of the Line Side Converter

The line side converter has to transmit the active power from the DC-link to the grid so that the DC-link voltage is kept constant. The corresponding controller and converter model is shown in the upper part of Fig. 11.

The output is the active current which is injected into the grid node. Depending on the software used, this current can be converted into an equivalent power. The reactive current is kept constant in the model shown in Fig. 11. However, during grid faults it is preferable to use line side converter to provide reinforced voltage support to the grid. For this purpose, different strategies are applicable, which are not discussed in this paper.

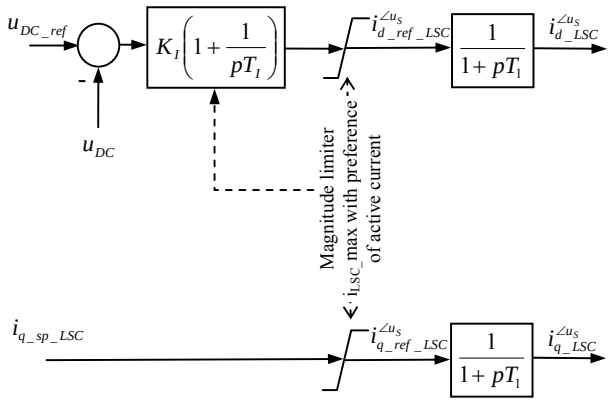

Fig. 11. Block diagram of line side converter model

VIII. Simulation Results

The following simulation results demonstrate the capability of the enhanced model introduced in this paper. As an example, the behavior of a typical DFIG wind turbine (2 MW) following a grid short circuit of 300 ms duration has been simulated. The wind turbine is connected to the 110-kV-network through two step-up transformers. The grid short circuit is simulated by a voltage dip at the 110-kV connection point from 100% to 15% at t=0 s. The DFIG system is equipped with a DC-chopper in order to avoid repeated crowbar switching. Fig. 12. provides a complete overview about the behavior of the DFIG and the associated converter during the short circuit period. All variables shown in the figures are given in p.u. Please note that according to the sign conventions used, the generated active power and capacitive reactive power are negative.

Due to the fast rise of the DC-link voltage the rotor side converter is stopped and the crowbar is switched on already after a few milliseconds. At t = 0.07 s the crowbar is switched off already and at t = 0.12 s rotor side converter is activated again, so that active and reactive currents can be controlled. Because the voltage is still low at this point, enforced reactive current is fed to the grid according to the grid code requirements. Operation modes alternate from mode 1) ('normal', t<0) to mode 4) at t = 0, to mode 2) at t>0 , , to mode 3) at t > 0.07 s and back to mode 1) at t >= 0.12 s. Note that currents and fluxes calculated by ROM/E model show alternating components in rotating reference frame, i.e. DC-components in stationary reference frame. Currents and fluxes calculated by the ROM [1] contain no alternating components. As can be seen, the DC-link voltage is largely influenced by this alternating component.

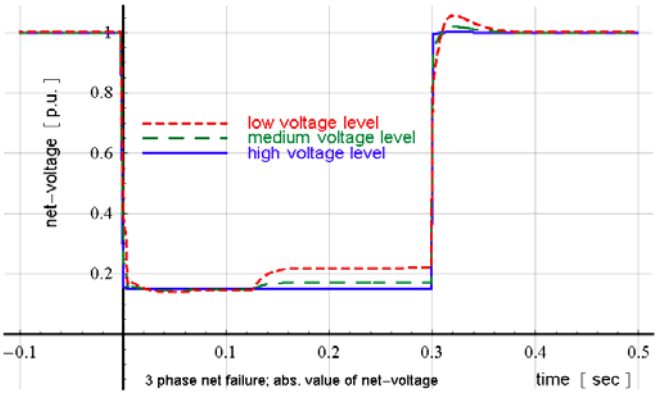

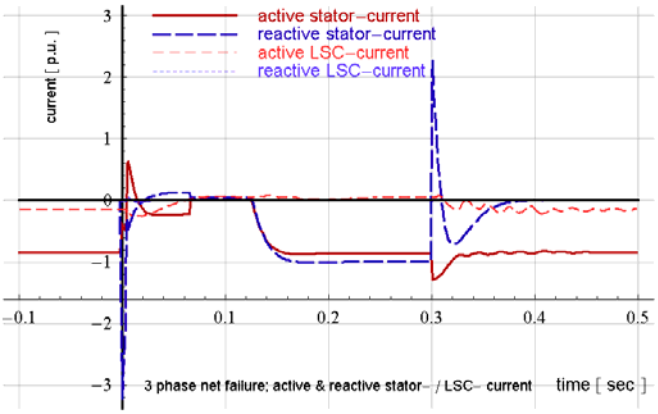

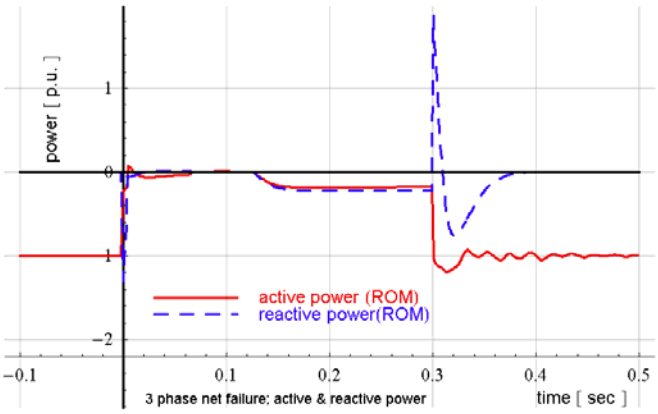

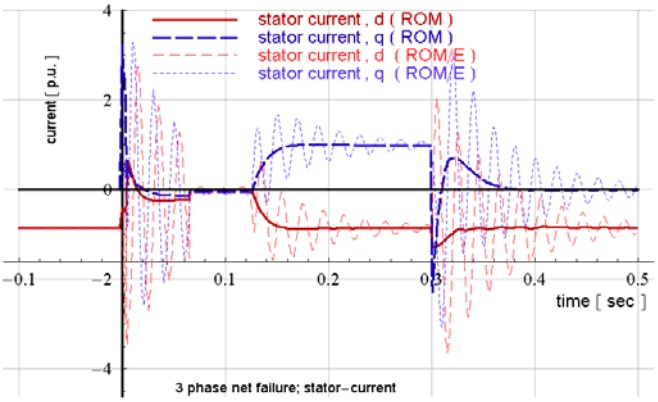

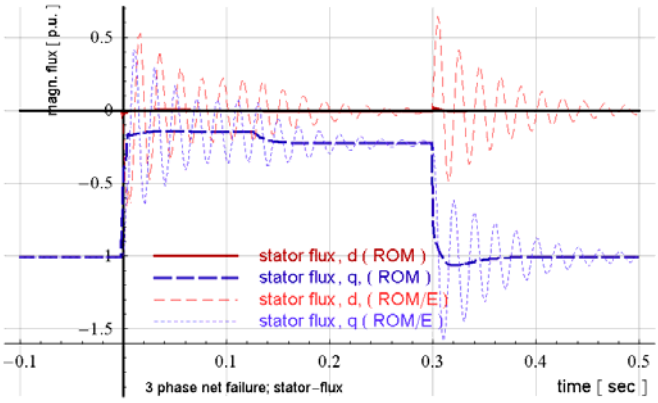

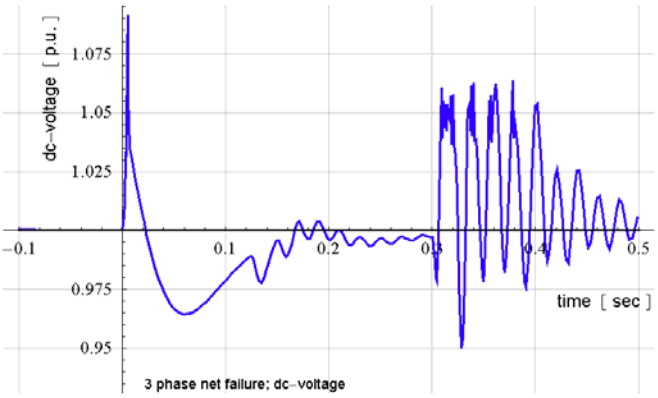

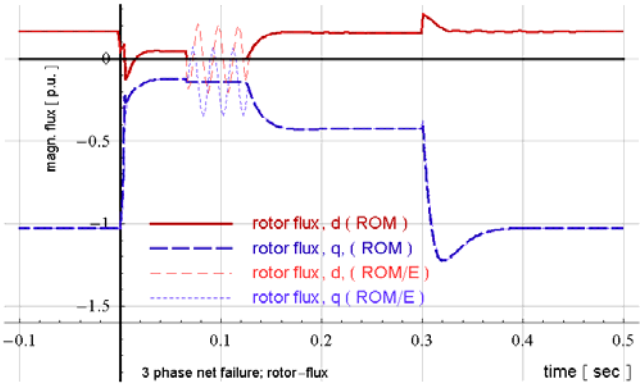

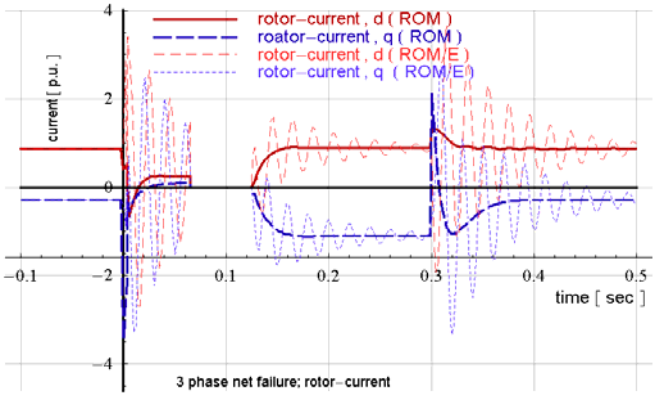

Fig. 12. First part - continuation on the next page

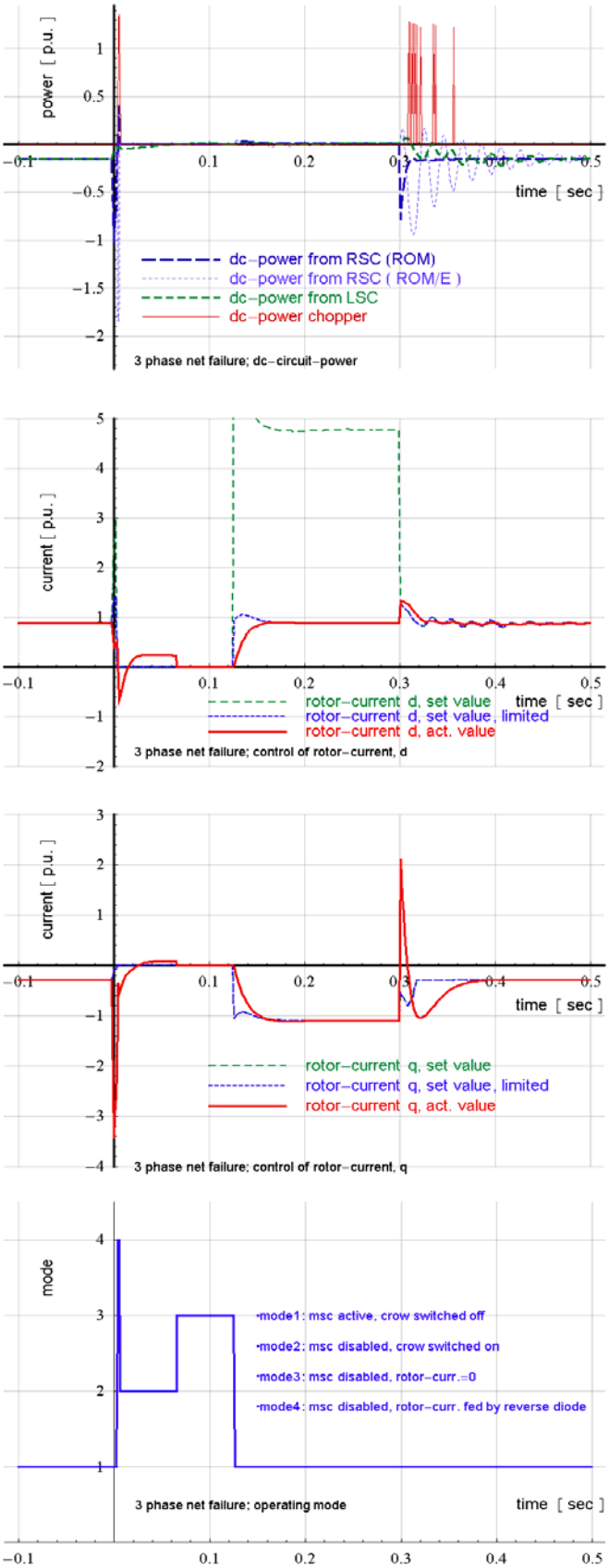

Fig. 12. Behavior of the DFIG following a voltage dip from 100% to 15% in the 110kV connection point

IX. Conclusions

The proposed model extension allows the simulation of the true sequence of the DFIG-response to grid faults by using basically the reduced order models (stability model) and the corresponding simulation algorithm. The grid is modeled in this approach by algebraic equations, so that the simulation performance is much better than the alternative instantaneous value calculation based on full order models for both DFIG and grid as well. With the proposed approach the alternating components of the rotor current are considered, so that the converter DC-link can be modeled realistically. Consequently, it is possible to consider the correct response of converter control and crowbar switching to voltage sags caused by grid faults. When the crowbar is switched on, the DFIG operates as a conventional slip-ring induction machine and becomes a reactive power consumer. It is expected that in the next years several wind farms with thousands of megawatts will go into operation [2]. Therefore, it is essential to consider the true control sequence and crowbar switching of DFIG-based wind turbines when simulating power system dynamic behavior. Moreover, the paper provides simulation results suited not only for model verification but also for demonstrating the behavior of the DFIG and the corresponding control system during fault.

X. References

[1] I. Erlich, U. Bachmann, “Grid code requirements concerning connection and operation of wind turbines in Germany”, Power Engineering Society General Meeting, 2005. IEEE, June 12-16, 2005 Page(s):2230 – 2234

[2] I. Erlich, W. Winter, A. Dittrich, “Advanced Grid Requirements for the Integration of Wind Turbines Into the German Transmission System” Power Engineering Society General Meeting, 2006. IEEE, June 18-22, 2006, Montreal

[3] I. Erlich, F. Shewarega, “Modeling of Wind Turbines Equipped with Doubly-Fed Induction Machines for Power System Stability Studies”, PSCE, October 29 – November 1, 2006, Atlanta 2

XI. BIOGRAPHIES

Jörg Kretschmann (1958) received his Dipl.-Ing. degree in electrical engineering from the Technical University Berlin, Germany, in 1986. In the period of 1986 to 1988 he worked for engineering department of AEG-Kanis in Essen, manufacturing of synchronous generators up to 200 MVA. Since 1988 he is with SEG GmbH & Co. KG, Kempen/Germany, as a design engineer for speed-variable applications: uninterruptible power supply, shaft alternators, DFIG for wind turbines. His main field is simulation of power converter systems, design of power components, passive grid-filter.

Holger Wrede (1971) received his Dipl.-Ing. degree in electrical engineering from the Technical University Braunschweig, Germany, in 1998. From 1998 to 2004 he joined the Institute for Electrical Power Engineering and Power Electronics of the Ruhr-University Bochum, Germany, where he worked on FACTS devices, power quality as well as compensation strategies and received his PhD degree in 2004. Since 2004 he is with SEG GmbH & Co. KG, Kempen/Germany, presently manager of the group Innovation / Converter Technology and responsible for system designs and simulations, control strategies and patents. He is a member of IEEE

Stephan Müller-Engelhardt (1967) received his Dipl.-Ing. degree in electrical engineering from the University Hannover, Germany, in 1997. Since 1997 he is with SEG GmbH & Co. KG, Kempen/Germany, as a design engineer for speed-variable applications: DFIG for wind turbines, uninterruptible power supply, shaft alternators. His main fields are controller design, system simulation and application software design for power converter systems.

Istvan Erlich (1953) received his Dipl.-Ing. degree in electrical engineering from the University of Dresden/Germany in 1976. After his studies, he worked in Hungary in the field of electrical distribution networks. From 1979 to 1991, he joined the Department of Electrical Power Systems of the University of Dresden again, where he received his PhD degree in 1983. In the period of 1991 to 1998, he worked with the consulting company EAB in Berlin and the Fraunhofer Institute IITB Dresden respectively. During this time, he also had a teaching assignment at the University of Dresden. Since 1998, he is Professor and head of the Institute of Electrical Power Systems at the University of Duisburg-Essen/Germany. His major scientific interest is focused on power system stability and control, modelling and simulation of power system dynamics including intelligent system applications. He is a member of VDE and senior member of IEEE.